Published OnlineFirst on July 14, 2010 as 10.1158/0008-5472.CAN-10-0076

Integrated Systems and Technologies

Cancer Research

A Microfluidic Platform for Systems Pathology: Multiparameter Single-Cell Signaling Measurements of Clinical Brain Tumor Specimens

Jing Sun[1,2,3,4], Michael D. Masterman-Smith[1,2,3,4,6], Nicholas A. Graham[1,2,3,4], Jing Jiao[1,2,3,4], Jack Mottahedeh[6], Dan R. Laks[6], Minori Ohashi[1,2,3,4], Jason DeJesus[5], Ken-ichiro Kamei[1,2,3,4], Ki-Bum Lee[1,2,3,4], Hao Wang[1,2,3,4], Zeta T.F. Yu[1,2,3,4], Yi-Tsung Lu[1,2], Shuang Hou[1,2,3,4], Keyu Li[1,2,3,4], Max Liu[1,2,3,4], Nangang Zhang[1,2], Shutao Wang[1,2,3,4], Brigitte Angenieux[6], Eduard Panosyan[6], Eric R. Samuels[1,2,3,4,6], Jun Park[1,2], Dirk Williams[1,2,4], Vera Konkankit[7], David Nathanson[2,5,8], R. Michael van Dam[1,2,4], Michael E. Phelps[1,2,3,4,8], Hong Wu[1,2,3,4,8], Linda M. Liau[7,8], Paul S. Mischel[2,3,5,8], Jorge A. Lazareff[7,8], Harley I. Kornblum[2,6,8], William H. Yong[5,8], Thomas G. Graeber[1,2,3,4,8], and Hsian-Rong Tseng[1,2,3,4,8]

Abstract

The clinical practice of oncology is being transformed by molecular diagnostics that will enable predictive and personalized medicine. Current technologies for quantitation of the cancer proteome are either qualitative (e.g., immunohistochemistry) or require large sample sizes (e.g., flow cytometry). Here, we report a microfluidic platform—microfluidic image cytometry (MIC)—capable of quantitative, single-cell proteomic analysis of multiple signaling molecules using only 1,000 to 2,800 cells. Using cultured cell lines, we show simultaneous measurement of four critical signaling proteins (EGFR, PTEN, phospho-Akt, and phospho-S6) within the oncogenic phosphoinositide 3-kinase (PI3K)/Akt/mammalian target of rapamycin (mTOR) signaling pathway. To show the clinical application of the MIC platform to solid tumors, we analyzed a panel of 19 human brain tumor biopsies, including glioblastomas. Our MIC measurements were validated by clinical immunohistochemistry and confirmed the striking intertumoral and intratumoral heterogeneity characteristic of glioblastoma. To interpret the multiparameter, single-cell MIC measurements, we adapted bioinformatic methods including self-organizing maps that stratify patients into clusters that predict tumor progression and patient survival. Together with bioinformatic analysis, the MIC platform represents a robust, enabling *in vitro* molecular diagnostic technology for systems pathology analysis and personalized medicine. *Cancer Res; 70(15); OF1–11.* ©2010 AACR.

Introduction

Technologies for the molecular diagnosis of cancer are rapidly changing the clinical practice of oncology (1, 2). As knowledge about the molecular basis of cancer increases, the development of tools capable of multiple, inexpensive biomarker measurements on small amounts of clinical tissue will be essential for the success of clinical trials, both to permit stratification of patients into groups most likely to benefit from targeted therapeutics and to evaluate the efficacy of such drugs on their molecular target.

For solid tumors, standard diagnostic methods rely on qualitative tissue immunohistochemistry (IHC; ref. 3). Unfortunately, a wide range of variables limit quantification of IHC data (4), and multiparametric analyses through IHC are technologically challenging and rarely used clinically. Thus, histologic analysis provides only limited insight into the molecular classification of tumors (5). In contrast, flow cytometry permits quantitative measurement of multiple proteins in individual cells (6), but its high sample/reagent consumption generally limits its diagnostic use to hematologic cancers (7). Therefore, molecular diagnosis of solid tumors necessitates a miniaturized platform featuring specimen economy and sensitive multiparametric measurement capabilities.

Glioblastoma multiforme (GBM) is the most lethal form of adult brain cancer and exhibits extensive molecular intertumoral and intratumoral heterogeneity (8). The phosphoinositide 3-kinase (PI3K)/Akt/mammalian target of rapamycin

Authors' Affiliations: [1]Crump Institute for Molecular Imaging, [2]Department of Molecular and Medical Pharmacology, [3]Institute for Molecular Medicine, [4]California NanoSystems Institute, [5]Department of Pathology and Laboratory Medicine, [6]Department of Psychiatry, [7]Department of Neurosurgery, and [8]Jonsson Comprehensive Cancer Center, University of California at Los Angeles, Los Angeles, California

Note: Supplementary data for this article are available at Cancer Research Online (http://cancerres.aacrjournals.org/).

J. Sun, M.D. Masterman-Smith, N.A. Graham, and J. Jiao, as well as T.G. Graeber and H-R. Tseng, contributed equally to this work.

Corresponding Authors: Thomas G. Graeber, University of California Los Angeles, 570 Westwood Plaza, CNSI 4341, Los Angeles, CA 90095. Phone: 310-206-6122; Fax: 310-206-8975; E-mail: tgraeber@mednet.ucla.edu or Harley I. Kornblum; Email: hkornblum@mednet.ucla.edu or William H. Yong; E-mail: wyong@mednet.ucla.edu or Hsian-Rong Tseng; E-mail: hrtseng@mednet.ucla.edu.

doi: 10.1158/0008-5472.CAN-10-0076

(mTOR) signaling pathway is frequently deregulated in GBM (8), often by overexpression of the epidermal growth factor receptor (EGFR) or other receptor tyrosine kinases (9, 10) and/or loss of the *PTEN* tumor suppressor (10, 11), leading to activation of the downstream effectors Akt and mTOR. The promise of targeted PI3K pathway inhibitors has led to some clinical improvement in patients (12), but therapeutic efficacy has been limited to a relatively small cohort of GBM patients (13, 14). Future development of successful targeted therapeutics for heterogeneous solid tumors like GBM will require the ability to detect molecular subsets that can guide appropriate patient selection in clinical trials (15).

Microfluidics exhibits intrinsic advantages of minimal sample/reagent usage, operational fidelity, high throughput, cost efficiency, and precise control over reagent and sample delivery to microscale environments (16). These microscale technology platforms are finding application in biological assays, including stem cell culture (17), gene expression (18), chromosomal analysis (19), and proteomics (20–23). Microfluidic platforms capable of single-cell analysis are also evolving, including a recent platform that allows single-cell interrogation of signaling networks in cultured cell lines (24). Given the clinical need for improved *in vitro* molecular diagnostic technologies that can characterize heterogeneity at the single-cell level in primary brain tumor biopsies, we combined the advantages of microfluidics (16) and microscopy-based cytometry (25) to develop the microfluidic image cytometry (MIC) platform.

Here, we use the MIC platform to show simultaneous, single-cell quantification of four signaling proteins (EGFR, PTEN, phospho-Akt, and phospho-S6) within the PI3K/Akt/mTOR signaling pathway. We show clinical application of the MIC technology by analyzing a panel of 19 human brain tumor biopsies (including both GBMs and low-grade brain tumors) and validate our MIC measurements with clinical IHC protocols. To compare the single-cell multiparameter MIC data sets with clinical outcome measures, we adapt bioinformatic methods, including self-organizing maps (SOM; ref. 26), to stratify tumor specimens into clusters. We found that these clusters correlate with tumor progression and patient survival. Therefore, the MIC platform represents a novel *in vitro* molecular diagnostic technology that will enable systems pathology analysis of solid tumors and patient stratification for personalized medicine.

Materials and Methods

Fabrication of the cell array chips

The cell array chip consists of 24 (3 × 8) cell culture chambers, each with dimensions of 8 mm (*l*) × 1 mm (*w*) × 120 μm (*h*) for a total volume of 960 nL. The cell array chip was fabricated by direct attachment of a polydimethylsiloxane (PDMS)-based microfluidic component onto a commercial poly-L-lysine (PLL)–coated glass slide (Polysciences) using an adhesive PDMS layer (Supplementary Fig. S1). The PDMS-based microfluidic component was fabricated by soft lithography methods using a silicon wafer replicate of photolithographically defined microchannel patterns. Cells, culture media, and reagents were introduced into the cell array chips by an electronic, handheld pipette (Thermo Fisher Scientific).

Reagents, cell lines, and tissue culture

The human glioblastoma cell line U87 was purchased from the American Type Culture Collection. All U87 cell lines (U87-PTEN, U87-EGFR, U87-PTEN-EGFR; ref. 33) were routinely maintained in DMEM containing 10% fetal bovine serum and 1% penicillin/streptomycin (Invitrogen). Erlotinib was purchased from LC Laboratories, and rapamycin and human recombinant EGF were from Sigma. For loading into microfluidic channels, U87 cells were dissociated using TrypLE (Invitrogen), pelleted, and resuspended at a density of 250 to 500 cells/μL. Two microliters of the U87 cell suspension were loaded into each microfluidic channel (Supplementary Fig. S2). Chips were then placed in a 10-cm Petri dish with 1 mL double-distilled water (ddH_2O) and incubated in a 5% CO_2, 37°C incubator for 16 hours before drug treatment and on-chip immunocytochemistry (ICC). Cells were treated with 20 μmol/L erlotinib for 48 hours, 20 nmol/L rapamycin for 48 hours, or 10 ng/mL EGF for 30 minutes.

Human tumor specimens

All patients were consented with approved University of California at Los Angeles (UCLA) Institutional Review Board protocols. Patient tumors were brought directly from neurosurgery suites of Ronald Reagan UCLA Medical Center upon resection and placed on ice for rapid portioning by the attending neuropathologist (WHY). Tumor portions were washed in PBS, minced with a scalpel blade, and dissociated into single-cell suspensions by TrypLE enzymatic digestion and gentle trituration, followed by a Percoll purification to remove cellular debris and red blood cells (Supplementary Methods; ref. 28). Tumor cells were filtered through a 40-μm single-cell strainer (Becton Dickinson) and loaded at a density of ~100 to 1,000 cells/μL into PLL-coated chips and centrifuged to facilitate cell attachment. Chips were then placed in a 10-cm Petri dish with 1 mL ddH_2O and placed in 5% CO_2, 37°C incubator for 15 minutes to allow cell attachment before on-chip ICC.

On-chip immunocytochemistry

On-chip ICC involves cell fixation (4% paraformaldehyde for 15 minutes at room temperature), washing with PBS, cell permeabilization (0.3% Triton X-100 for 15 minutes at room temperature), washing, blocking (10% normal goat serum, 3% bovine serum albumin, and 0.1% *N*-dodecyl-β-maltodextrose for 12 hours at 4°C), immunolabeling (12 hours at 4°C) followed by washing, and 4′,6-diamidino-2-phenylindole staining before microscopy-based image cytometry. For immunolabeling, an optimized mixture of fluorophore-conjugated antibodies was prepared by mixing anti-EGFR (BD Pharmingen) labeled with LiCor/HiLyte Fluor 750 (Dojindo Molecular Technologies), phycoerythrin-conjugated anti-PTEN (BD Biosciences), Alexa Fluor 647–conjugated anti–pS473-AKT (Cell Signaling Technology),

and Alexa Fluor 488–conjugated anti-pS235/S236-S6 (Cell Signaling Technology).

Image acquisition and processing

Following image acquisition, MetaMorph (Molecular Devices, version 7.5.6.0) was used to quantify fluorescent signals in individual cells using the Multi-Wavelength Cell Scoring module. Fluorescence intensity values were normalized by the cell spread surface area, and background staining was subtracted (Supplementary Methods). Data were logarithmically transformed to create Gaussian-like distributions for subsequent analysis.

IHC methods

IHC was carried out as previously described (29). Briefly, formalin-fixed, paraffin-embedded tissue samples were sectioned, stained with a PTEN monoclonal antibody (clone 6H2.1, DAKO), and counterstained with Mayer's hematoxylin. PTEN staining was analyzed and scored according to established methods (14).

Bioinformatics analysis

To analyze the single-cell multiparameter MIC measurements, SOMs were created in R using the *Kohonen* package of Wehrens and Buydens (30). Briefly, a SOM grid consists of a set of units characterized by a vector of four values (EGFR, PTEN, pAkt, and pS6), and MIC measurements are mapped to the SOM grid based on similarity to the characteristics of the SOM units. The vectors characterizing the SOM grid were trained using an input data set representing the global measurement space (Supplementary Methods). After training, each tumor specimen was individually mapped to the SOM grid and plotted as the frequency of cells mapping to each SOM unit. To cluster the SOM mappings of the tumor specimens, we calculated a neighborhood frequency (the sum of the frequencies for a SOM unit and its neighbors, Supplementary Fig. S12A), and these values were subjected to unsupervised hierarchical clustering using the average-linkage method based on the Pearson correlation (31). Data were visualized using Java Treeview (32).

Patient survival/progression analysis

Overall survival was determined as the interval between the date of surgery when the tumor specimen was obtained for MIC analysis and the last date of known clinical follow-up or date of death using death certificates and the social security index. Time to progression was determined by the duration of progression-free survival from the date of surgery until recurrence, death, or, if progression-free, until the last follow-up date. Overall survival and time-to-progression were related to the SOM-derived clusters using a Cox proportional hazards model (Stata 8.0; ref. 33). This analysis was performed in the full patient cohort, comparing the patients belonging to each SOM-derived cluster against the remaining patients. All P values were two-tailed, and $P < 0.05$ was considered significant. Survival distributions were presented as Kaplan-Meier plots.

Results

Design of the MIC platform

To develop a molecular diagnostic tool for multiparameter pathology analysis of solid tumor specimens, we designed a simple monolithic microfluidic device to enable quantitative ICC. The MIC platform integrates (*a*) a PDMS-based microfluidic cell array chip for accommodating up to 24 cellular samples and performing ICC (Fig. 1A) with (*b*) fluorescence microscopy and imaging software for quantitative cytometry, followed by multiparameter pathology analysis (Fig. 1B). Chip fabrication uses soft lithography techniques, followed by direct attachment of the PDMS chip onto a PLL-coated glass slide using an adhesive PDMS film (Materials and Methods and Supplementary Fig. S1). Automated pipetting enables parallel cell culture and quantitative ICC on ~1,000 to 2,800 cells per sample (Supplementary Fig. S2), making the MIC platform ideal for highly efficient parallel measurement of up to 24 samples of less than 3,000 cells.

Optimization and validation of the MIC platform using model cell lines

Before testing the MIC platform on primary patient samples, we optimized ICC and microscopy-based cytometry protocols using the U87 GBM cell line and variants overexpressing EGFR, PTEN, or EGFR with PTEN (U87-EGFR, U87-PTEN, U87-PTEN-EGFR, respectively; ref. 27) to show reproducible quantification of EGFR, PTEN, pAKT, and pS6 expression/phosphorylation levels. Although some GBMs often overexpress a constitutively active mutant form of EGFR (EGFRvIII), we used an antibody that recognizes EGFR but not EGFRvIII[9] because intratumoral expression of wild-type EGFR is typically more extensive than this mutant form (34). On-chip growth curves confirmed that the microfluidic environment did not affect proliferation rates compared with off-chip cell culture (Supplementary Fig. S3). ICC and image processing protocols were developed by (*a*) optimization of antibody concentrations and confirmation of minimal cross-reactivity among antibodies (Supplementary Fig. S4; ref. 35); (*b*) standardization of microscopy parameters (i.e., exposure, light source, gain; Supplementary Methods); and (*c*) demonstration of measurement reproducibility (Supplementary Fig. S5). These data show that the optimized MIC protocols allow reproducible, simultaneous, single-cell measurement of EGFR, PTEN, pAkt, and pS6 in cultured cell lines.

Before the application of the MIC platform to analyze primary patient samples, we established the dynamic range of MIC measurement for EGFR, PTEN, pAKT, and pS6. Using U87 cell lines expressing EGFR and/or PTEN, the MIC platform showed at least an order of magnitude signal separation between positive and negative controls for all four signaling proteins (Fig. 2A). Because microfluidics should offer highly

[9] J. Sun and H-R. Tseng, unpublished observation.

reduced sample requirements compared with traditional methods, we also evaluated specimen economy and found that traditional Western blotting requires 2 to 3 orders of magnitude more cells than MIC analysis to yield similar results (Supplementary Fig. S6). To assess the sensitivity of MIC measurements, we used *Pten* wild-type and *Pten* knockout MEF cell lines (36), and verified that MIC can detect differences in endogenous PTEN expression (Supplementary Fig. S7). Therefore, MIC offers a highly sensitive platform for simultaneous single-cell quantification of the PI3K/Akt/mTOR pathway with microscopic sample sizes.

Because solid tumors like GBM exhibit significant intratumoral heterogeneity (8), we next tested the ability of the MIC platform to resolve heterogeneous populations of cancer cells by analyzing a mixture of U87 isogenic cell lines overexpressing EGFR and/or PTEN using the MIC platform. Qualitative examination of the four-color overlay image revealed the expected differences in protein expression within the cell mixture (Fig. 2B). Quantitative analysis of this U87 cell mixture using a two-dimensional contour plot revealed four clusters clearly identifying the four U87 cell lines (Fig. 2C). These results were confirmed by a similar analysis of the four individually stained cell lines (Supplementary Fig. S8), thus demonstrating that the MIC platform can quantitatively discriminate distinct molecularly defined subsets within a heterogeneous cell mixture.

Validation of the MIC platform using clinical tumor samples

Having shown that the MIC platform can quantitatively characterize heterogeneous mixtures of cultured cells, we next tested the utility of the MIC for clinical molecular diagnostics of human tumor tissue. To allow for analysis of solid tumors, we adapted an established tissue processing protocol for dissociation of tumor cells into a single-cell suspension and optimized critical aspects of sample preparation to ensure reproducibility (Supplementary Information; ref. 28). With this protocol, we then analyzed a cohort of 19 clinical brain tumor specimens, including GBMs and several low-grade tumor types such as oligoastrocytomas and oligodendriomas (Supplementary Table S1). Notably, MIC analysis requires only 1,000 to 2,800 cells, far fewer than would have been necessary for analysis by population average techniques such as Western blotting. We verified that MIC measurements did not correlate with either the total number of cells measured or the number of cells per MIC channel (data not shown). Using rank-based graphs of MIC measurements from a subset of tumors, we first demonstrated extensive intratumoral and intertumoral heterogeneity in single-cell expression levels of EGFR, PTEN, pAkt, and pS6 (Fig. 3A; Supplementary Fig. S9). These data show that the MIC platform can quantitatively capture the molecular heterogeneity characteristic of GBM and other brain tumor types (8).

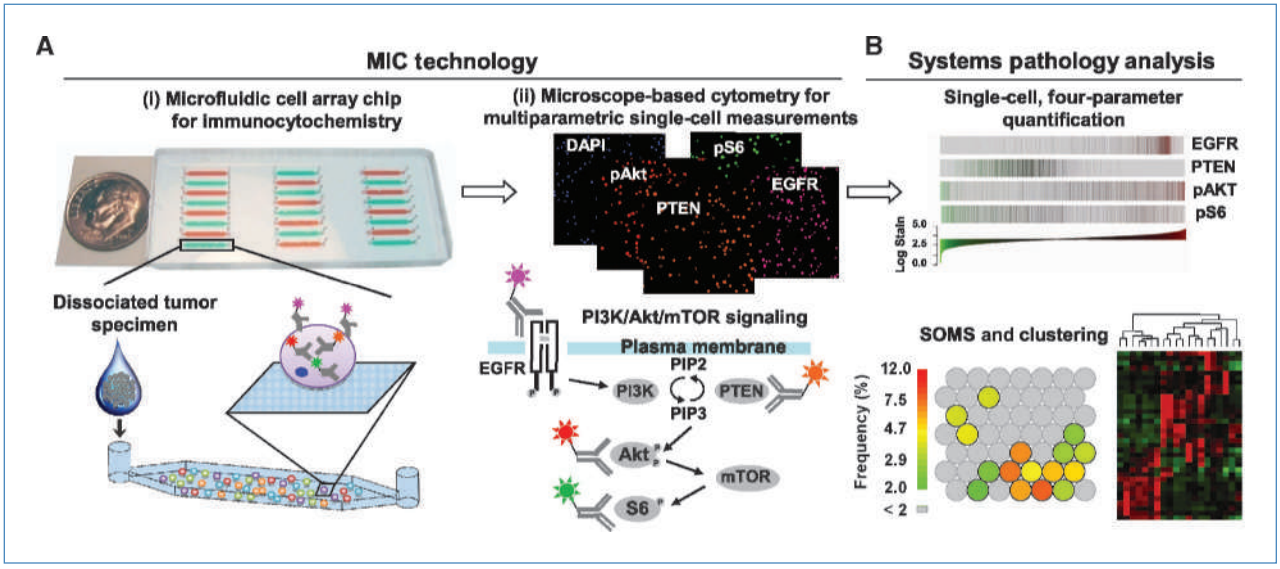

Figure 1. Conceptual summary of the MIC technology for systems pathology analysis of clinical brain tumor specimens. A, the MIC technology is composed of (I) a cell array chip with 24 microfluidic channels (here alternately loaded with red and green food dyes to aid visualization) for accommodating dissociated tumor specimens and performing ICC, and (II) image acquisition and cytometry analysis by fluorescent microscopy to quantitatively measure multiple signaling molecules in individual cells. In our study, four signaling proteins and phosphorylation states (EGFR, PTEN, pAkt, and pS6) within the oncogenic PI3K/Akt/mTOR signaling pathway were immunostained with fluorophore-conjugated antibodies [i.e., anti-EGFR (purple), anti-PTEN (orange), anti-pAKT (red), and anti-pS6 (green)]. B, systems pathology analysis using SOMs. MIC analysis yields complex, single-cell multiparameter data sets, as represented by the rank-based graphs (top), where single-cell data are sorted from low to high levels of expression/phosphorylation and represented as vertical bars that are shown on a green to red color scale to indicate the expression/phosphorylation intensity. Projecting MIC measurements onto a SOM (bottom) reduces the data dimensionality and visually summarizes the single-cell multiparameter MIC data sets to qualitatively evaluate signal transduction phenotypes. Hierarchical clustering can then stratify SOM maps of patient specimens into molecular signatures, which may guide the implementation of personalized molecular therapy.

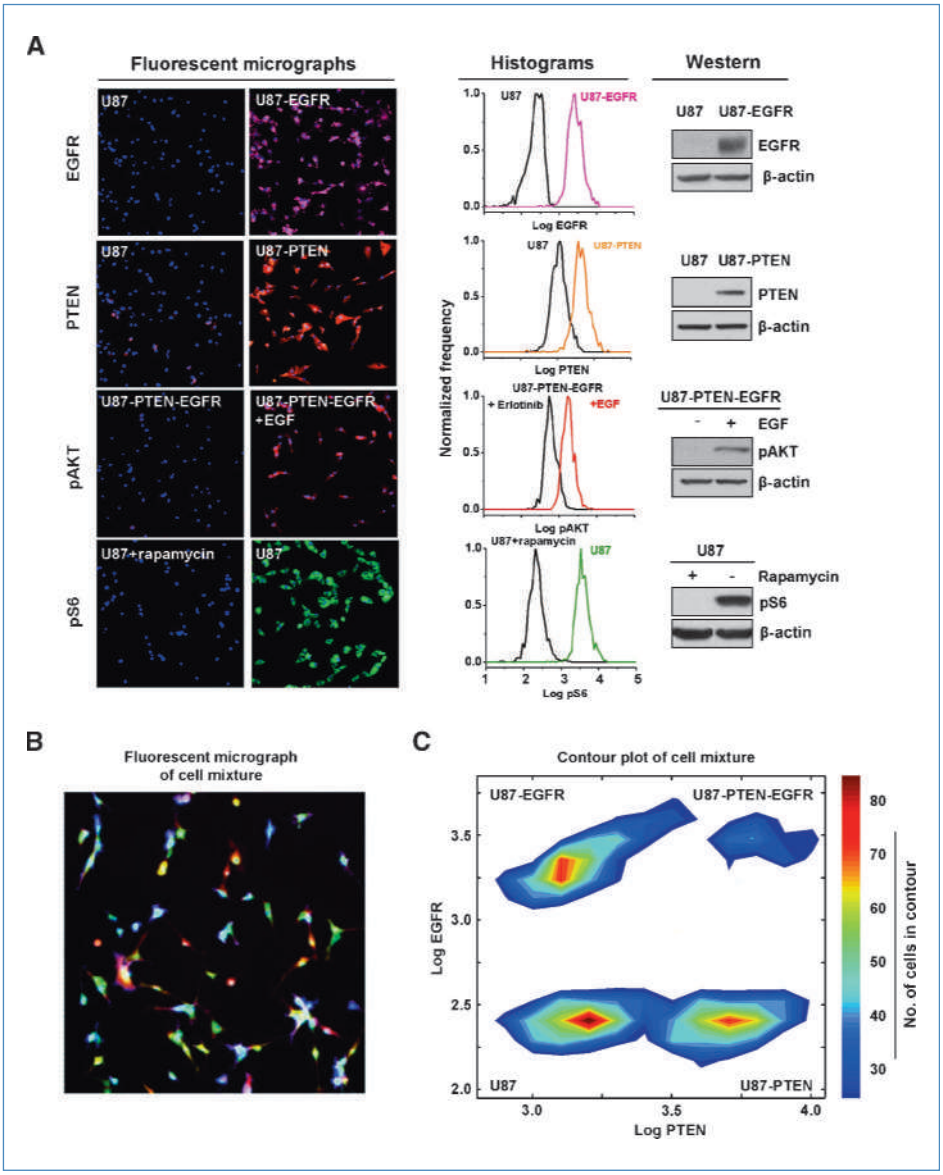

Figure 2. Optimization and validation of the MIC technology using brain tumor cell lines. A, four pairs of cell lines and treatments (U87 versus U87-EGFR, U87 versus U87-PTEN, serum-starved U87-PTEN-EGFR versus EGF-treated U87-PTEN-EGFR, and rapamycin-treated U87 versus U87) were used to show the dynamic range of the MIC technology for quantification of EGFR, PTEN, pAkt, and pS6. Left, fluorescent micrographs of ICC-treated cells; middle, histograms of the dynamic ranges of MIC measurement for the four signaling proteins and phosphorylation states in individual cells; right, validation of the expression/phosphorylation levels of EGFR, PTEN, pAkt, and pS6 by Western blotting. β-Actin is included as an equal loading control. B and C, MIC analysis of cellular heterogeneity within a cell mixture. MIC analysis was performed on a cell mixture containing an approximately equal ratio of four U87 cell lines (U87, U87-EGFR, U87-PTEN, and U87-PTEN-EGFR). B, a fluorescent micrograph of the U87 cell mixture demonstrating the expected heterogeneity in protein expression/phosphorylation. C, MIC measurements of the U87 cell mixture (~4,000 cells) plotted on a two-dimensional contour plot, where color represents the number of cells present in each contour level, confirm the presence of four clusters. Although U87-PTEN-EGFR cells look underrepresented in the cell mixture, analysis of individually stained cell lines revealed that this appearance is due to a broader distribution of PTEN expression in U87-PTEN-EGFR cells than in the other isogenic cell lines (Supplementary Fig. S8C).

Because PTEN expression is routinely measured by IHC in the clinic, we compared our MIC measurements to clinically practiced IHC protocols (Fig. 3B; Supplementary Table S1; ref. 14). Although quantitative single-cell MIC data are fundamentally different than qualitative IHC scoring, we found that the percentage of cells expressing PTEN as scored by IHC corroborated the MIC measurements for eight of nine cases. The discrepancy between clinical IHC and MIC measurements of PTEN expression in patient 7 may be due to the extremely heterogeneous nature of this sample, where evidence of foamy macrophages, necrosis, and normal brain were found. Thus, clinical IHC validated the accuracy of our quantitative, single-cell MIC measurements.

Multiparameter pathology analysis of human tumor specimens

Meaningful interpretation of the multiparameter single-cell MIC measurements from resected brain tumors requires the application of bioinformatic techniques. To facilitate systems pathology analysis of these human brain tumor specimens, we adapted SOMs (26), an unsupervised learning method that has found wide application in analysis of complex biological data sets (37–39). SOMs project high-dimensional data onto a two-dimensional grid where the topological location of points represents similarity or dissimilarity (Supplementary Fig. S10), thus placing highly similar multidimensional objects in close proximity to each other on the SOM grid (30). When applied to MIC measurements, each SOM unit represents a characteristic set of EGFR, PTEN, pAkt, and pS6 expression levels (Fig. 4A). For each patient sample, a color scale indicates the frequency of cells that map to the SOM units, and the resulting pattern provides a visual summary of the similarities, dissimilarities, and the degree of heterogeneity within a set of multiparameter, single-cell MIC measurements.

Examining SOM mappings for all 19 clinical brain tumor specimens, we again observed striking intertumoral and intratumoral heterogeneity (Fig. 4B), as previously shown using single-parameter measurements (Fig. 3A; Supplementary Fig. S9). In addition, we found that the degree of

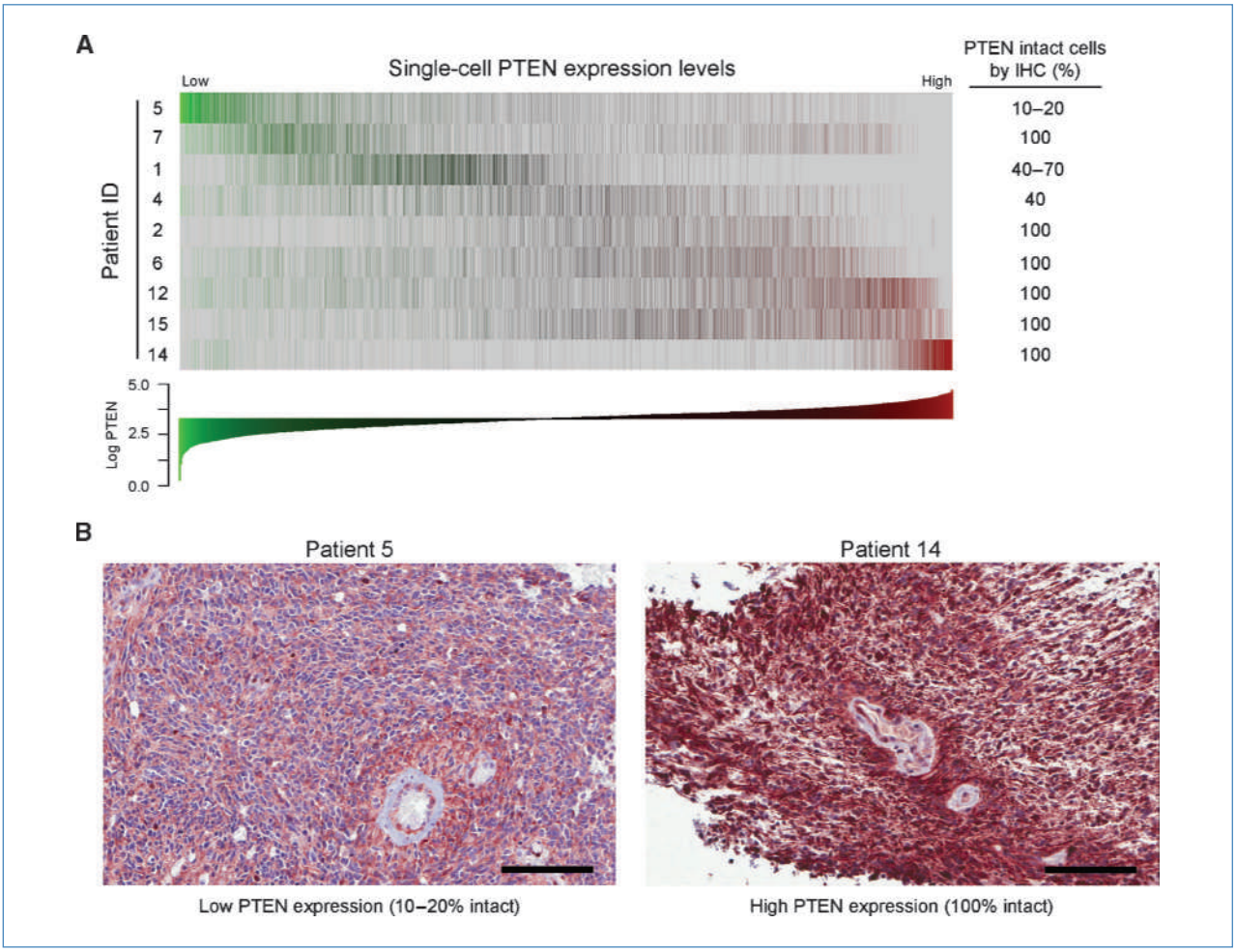

Figure 3. MIC analysis reveals heterogeneity of PTEN expression in human brain tumor specimens and is validated by clinical IHC measurements. Dissociated human brain tumor cells (1,000–2,800 cells per tumor specimen) were stained for EGFR, PTEN, pAkt, and pS6 using the MIC technology. A, left, ranked graph of PTEN expression in human brain tumor specimens. Single-cell MIC measurements from nine tumor samples were ranked from lowest to highest PTEN expression and plotted on a ranked graph (Supplementary Methods), where each row corresponds to the indicated tumor sample and each vertical bar represents one cell. For cells belonging to the tumor sample on each row, the vertical bar was shaded from green to red to indicate low and high PTEN expression, respectively, as indicated in the scale bar. Notably, most tumors contain both cells expressing very low and very high levels of PTEN. Right, PTEN expression in the same tumor samples was measured using clinically practiced IHC protocols, and the percentage of cells scored as "PTEN intact," as indicated by no detectable decrease in PTEN expression comparison to endothelial cells, is reported (14). The IHC scoring and single-cell MIC measurements of PTEN expression show good qualitative agreement. B, representative IHC images of patients with low (patient 5, left) and high (patient 14, right) PTEN expression. Scale bars represent 100 μm.

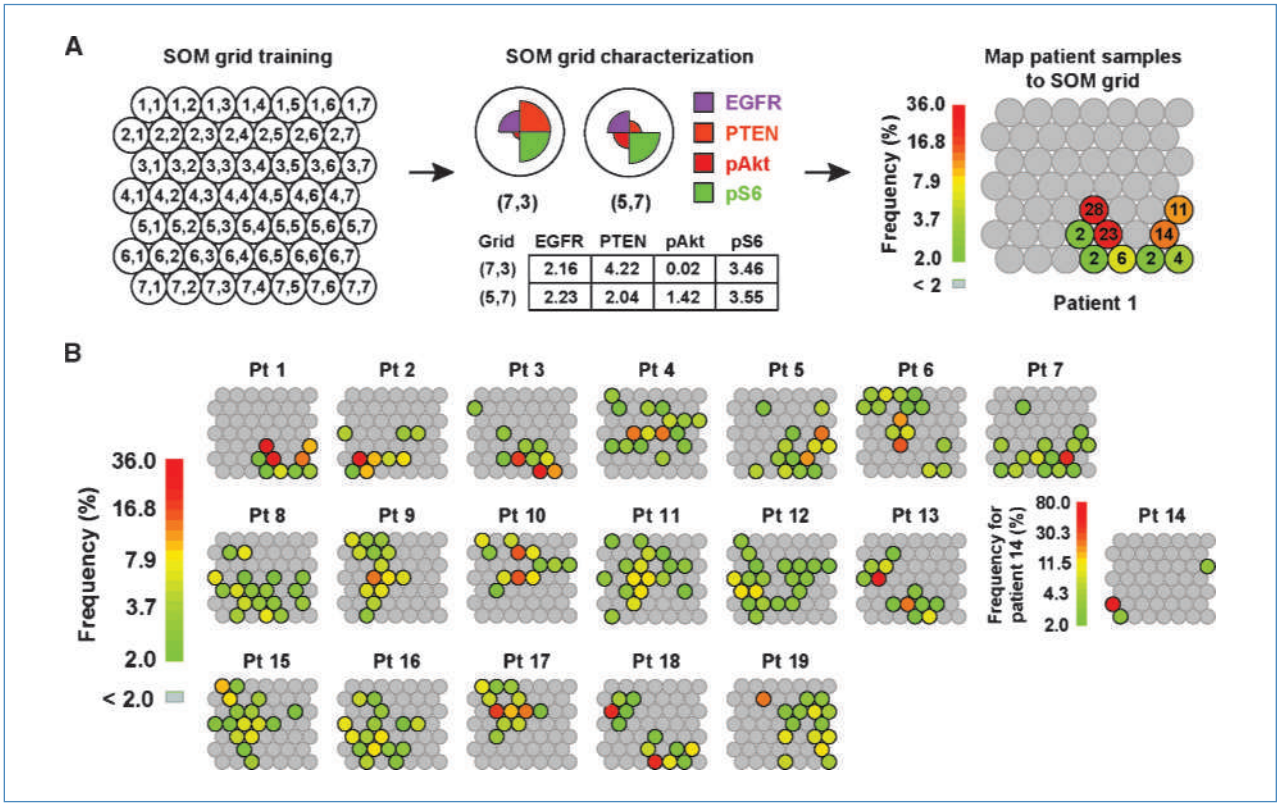

Figure 4. Characterization of human brain tumors by multiparameter SOM analysis reveals intertumoral and intratumoral heterogeneity. A, overview of the SOM method for analysis of MIC measurements. Left, a schematic of a 7 × 7 SOM with each SOM unit labeled with its address. This SOM grid is trained using single-cell four-parameter measurements of EGFR, PTEN, pAkt, and pS6. Center, after training, each SOM unit is described by a vector of EGFR, PTEN, pAkt, and pS6 values. Two representative SOM units are described in a piechart format and in a table (Supplementary Fig. S10). Right, each individual patient sample can be mapped to the SOM grid, and the frequency at which individual cells are assigned to each SOM unit is represented by a color scale. The numbers inside each SOM unit correspond to the frequency of cells mapped to that SOM unit for patient 1. B, SOM mappings for brain tumor patient cohort. Single-cell MIC measurements for 19 brain tumor patient (Pt) specimens were mapped to the SOM grid, revealing heterogeneity both across patients and within individual samples. Because patient 14 exhibited a uniquely homogeneous SOM mapping, this map is depicted using its own color scale.

intratumoral heterogeneity could be quantitatively assessed by varying the size of the SOM grid (Supplementary Fig. S11), with homogeneous tumors (e.g., patients 1, 3, and 14) and heterogeneous tumors (e.g., patients 8, 11, and 12) exhibiting concentrated and dispersed SOM mappings, respectively. To test the possibility of using MIC-derived SOMs for patient stratification, we represented each SOM mapping as a neighborhood frequency vector (NFV, the sum of the frequency of cells mapped to a SOM unit and its surrounding neighbors; Fig. 5A; Supplementary Fig. S12A) and performed unsupervised clustering of the 19 patient-specific NFVs. Clustering of these NFVs revealed three predominant clusters of patient samples (Fig. 5B; Supplementary Fig. S12). Although cluster II was comprised only of GBMs, both clusters I and III exhibited mixed tumor type composition. We deconvoluted the original staining patterns that characterize each cluster to reveal expression/signaling phenotypes and found that cluster I (eight patient samples) exhibits medium EGFR, low PTEN, and high pS6 expression; cluster II (four patient samples) exhibits high expression of EGFR, PTEN, and pAkt; and cluster III (seven patient samples) exhibits low EGFR and pS6 expression. By ANOVA analysis, EGFR was the most discriminatory biomarker between the three clusters, followed in decreasing order by pS6, PTEN, and pAkt (Fig. 5B; Supplementary Fig. S12D). Thus, SOMs can serve as a technique for stratification of multiparameter, single-cell MIC measurements of clinical brain tumor specimens.

SOM mappings of human tumor samples correlate with patient survival and tumor progression

To assess the clinical significance of these groupings, we tested whether these MIC-derived clusters correlate with clinical outcome measures. Although the median duration between tumor resection and survival analysis was shorter (317 days) than the median survival time of GBM patients (~365 days; ref. 8), we found that cluster II was significantly associated with an increased hazard of patient death [hazard ratio (HR) >5.35, $P < 0.05$; Fig. 5C; Supplementary Fig. S13]. Conversely, cluster I was significantly associated with a decreased hazard of patient death (HR < 0.001, $P < 0.001$), and cluster III did not exhibit any significant difference in

overall survival. Analysis of progression-free survival showed similar trends to overall survival, although the HRs were not statistically different from the remaining cohort (Supplementary Fig. S13). This analysis shows the potential of the MIC platform for classification of molecularly defined patient subsets of clinical significance.

Discussion

The clinical diagnosis of cancer is being transformed from phenomenological descriptions to molecular, systems-based disease models. Quantitative, sensitive, and inexpensive single-cell molecular diagnostic measurements of precious

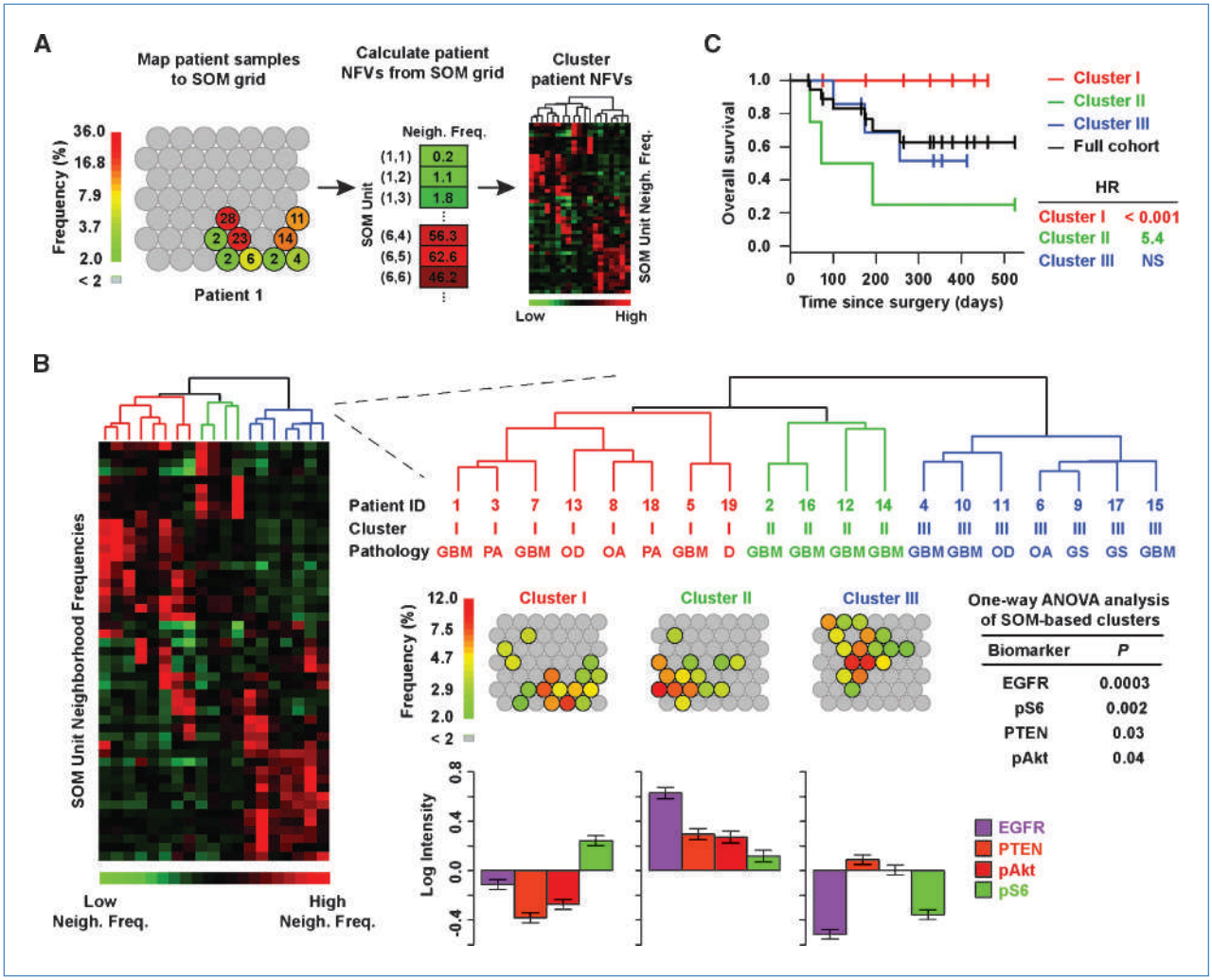

Figure 5. Multiparameter SOM analysis of human brain tumors permits patient stratification into clusters that predict clinical outcome. A, clustering of SOM mappings. Left, individual patient samples can be mapped to a SOM as described in Fig. 4A, where the color represents the frequency at which individual cells are assigned to each SOM unit. Center, to quantitatively compare SOM mappings from different patients, the neighborhood frequency (Neigh. Freq., the sum of the frequencies for a unit and its surrounding neighbors; Supplementary Fig. S12A) is calculated and arranged into a NFV. Right, the NFVs for each patient sample are clustered, and the output is represented by a heatmap where red and green indicate relative high and low neighborhood frequencies, respectively. B, clustering NFVs calculated from SOM mappings reveals distinct signatures of PI3K/Akt/mTOR pathway activity. NFVs representing the 19 tumor specimens were subjected to unsupervised hierarchical clustering, and the results were depicted using a heatmap where each row corresponds to a SOM unit and each column represents a tumor specimen. Red and green indicate relative high and low neighborhood frequencies, respectively. Tumor types are shown at right in the enlarged dendrogram for each patient (PA, pilocytic astrocytoma; D, dysembryoplastic neuroepithelial tumor; OA, oligoastrocytoma; OD, oligodendrioglioma; GS, gliosarcoma). Because the dendrogram indicated three predominant clusters, the average map and weighted signature for each cluster of patient samples were calculated. To assess which of the expression/phosphorylation levels contributed most to the multiparameter, SOM-based clustering, we performed an ANOVA analysis of the patient sample mean expression levels and found that EGFR was the most differentially expressed signaling/phospho-protein between the three SOM-based clusters (Supplementary Fig. S12C). C, SOM-based clustering of tumor specimens correlates with clinical outcome measures. Kaplan-Meier curves for overall survival of the entire patient cohort (black) and clusters I (red), II (green), and III (blue). Cluster II was significantly associated with an increased hazard of patient death ($P < 0.05$), whereas cluster I was significantly associated with a decreased hazard of patient death ($P < 0.001$; Supplementary Fig. S13, N.S., not significant).

clinical samples will both increase our knowledge of the etiology of cancer and enable the development and judicious application of targeted therapeutics (1, 2). Here, we report a new technology, MIC, which combines the advantages of microfluidics and microscopy-based cytometry to enable multiparameter pathology analysis of solid tumors. The design, application, and analysis of the MIC systems pathology platform represent a novel synthesis of several technological developments, including (*a*) microfluidic "chip" design to enable inexpensive, robust, multiparameter, single-cell quantitation of precious samples; (*b*) improved processing and handling of sensitive tumor samples; and (*c*) adaptation of bioinformatic methods to interpret high-dimensional data. Because of the demonstrated clinical need for molecular classification of gliomas (13, 14), we targeted the oncogenic PI3K/Akt/mTOR pathway in brain tumors of varying stages and pathologic states, including GBM.

Microfluidics has emerged as a promising platform for molecular diagnosis of clinical samples (2, 16), with demonstrated applications including the detection of chromosomal translocations (19), measurement of oncoprotein expression and phosphorylation (20), and biomarker measurements in serum and saliva (21, 22). Although integrated microfluidic devices have previously been used to dissect two-parameter dynamics of signal transduction in cultured cell lines (24), we have expanded the utility of microfluidic platforms to four-parameter *in vitro* molecular diagnosis using microscopic amounts of human clinical tissue. The MIC platform specifically addresses shortcomings of currently practiced clinical diagnostics, including the qualitative imprecision of IHC (3) and the high sample/reagent consumption requirements of flow cytometry (7).

The single-cell nature of these MIC measurements permitted novel characterization of intertumoral and intratumoral heterogeneity in solid tumors. As expected from an infamously heterogeneous tumor type like GBM, we observed a diversity of signaling phenotypes that would have been masked by population-average measurements (Figs. 3A and 4B). Although IHC-based analyses of tissue microarrays have enabled systems analysis of glioblastomas (29), these techniques offer only semiquantitative measurement of successive tissue slices, as opposed to simultaneous, single-cell quantification of multiple biomarkers. Much as flow cytometry has enabled single-cell phospho-proteomics in liquid and some solid tumors to identify cancer cell subsets that predict clinical outcome (40), we expect that further application of the MIC to solid tumors will reveal molecular signatures that are not measurable by population-average techniques (41).

The ability to discriminate and characterize molecular subsets within and between patients will be essential for efficacious use of effective targeted therapeutics in highly heterogeneous solid tumors like glioma (15), particularly given that one molecularly targeted drug, the EGFR kinase inhibitor erlotinib, proved effective only in a subset of patients expressing both the constitutively active EGFRvIII mutant and PTEN (14). Here, we have shown that bioinformatic analysis of MIC measurements can reveal molecular signatures that predict tumor progression and patient survival (Fig. 5C). Notably, cluster II exhibits an increased hazard of patient death, potentially because of high EGFR expression because EGFR is the most discriminatory biomarker between the clusters (Supplementary Fig. S12D) and high EGFR expression is negatively correlated with GBM patient survival outcome (42). Importantly, univariate survival analysis did not reveal significant correlation between any of the individual EGFR/PI3K/Akt/mTOR pathway components and patient survival, demonstrating the improved performance of the multiparameter signature approach. However, given the relatively small size of our patient cohort (19 patients), these SOM-based signatures will require validation in a larger, independent data set before full comparison to other established biomarker trends (43). Finally, although none of the patients included in this study were treated with targeted inhibitors against the PI3K/Akt/mTOR pathway (e.g., erlotinib or rapamycin; see Supplementary Table S1), future studies will be designed to identify links between the SOM-based stratification of patients described here and previously identified molecular signatures predictive of a positive response to targeted inhibitors (14).

Given the relatively short median duration between tumor resection and outcome analysis (317 days), we note that long-term follow-up studies on larger patient cohorts will be required to validate the clinical significance of MIC-derived, SOM-based molecular signatures. Nevertheless, the encouraging prognostic significance in a relatively small sample size shows the potential of integrating bioinformatic analysis with single-cell measurements to stratify solid tumor biopsies into clusters with clinical relevance. Future studies using the MIC platform will expand the number of measured biomarkers using additional fluorophores and quantum dots (44), in expectation that additional measured biomarkers will enable a more thorough systems analysis and permit further dissection of molecular subtypes and identification of biomarker signatures in GBM (e.g., PDGFR, IDH1, NF1, Notch; refs. 45, 46). As the number of measured biomarkers expands, the need for bioinformatic analysis techniques such as SOMs will become even greater.

In summary, we have developed MIC, a highly precise, reliable technology platform requiring microscopic amounts of reagents (~2 μL/channel) and samples (<3,000 cells) for multiparamater, quantitative single-cell systems pathology of solid tumors. Because of the flexible nature of the assay, we envision rapid application both to comparison of molecular endpoints pre- and post-treatment in clinical samples using fine-needle biopsies (47) and to analysis of *in vitro* prognostic models such as multipassage neurosphere cultures (48). Coupled with systems pathology analysis, the MIC technology platform represents one of the first emerging microtechnologies to provide meaningful correlations between measurements of minute patient samples and clinical prognosis. As such, the MIC platform represents a novel technology for quantitative multiparameter pathology to enable prospective studies integrating *in vitro* molecular diagnostics, systems analysis of disease, and patient stratification for personalized medicine (2, 5).

Disclosure of Potential Conflicts of Interest

No potential conflicts of interest were disclosed.

Grant Support

Department of Energy, NanoSystems Biology Cancer Center, UCLA Brain Tumor Translational Resource; H.I. Kornblum was supported by NIH National Institute of Neurological Disorders and Stroke NS052563; N.A. Graham is a postdoctoral trainee supported by the UCLA Tumor Biology Program United States Health and Human Services Ruth L. Kirschstein Institutional National Research Service Award T32 CA009056; and T.G. Graeber is an Alfred P. Sloan Research Fellow.

The costs of publication of this article were defrayed in part by the payment of page charges. This article must therefore be hereby marked *advertisement* in accordance with 18 U.S.C. Section 1734 solely to indicate this fact.

Received 01/12/2010; revised 05/19/2010; accepted 05/24/2010; published OnlineFirst 07/13/2010.

References

1. Papadopoulos N, Kinzler KW, Vogelstein B. The role of companion diagnostics in the development and use of mutation-targeted cancer therapies. Nat Biotechnol 2006;24:985–95.
2. Heath JR, Davis ME. Nanotechnology and cancer. Annu Rev Med 2008;59:251–65.
3. Cregger M, Berger AJ, Rimm DL. Immunohistochemistry and quantitative analysis of protein expression. Arch Pathol Lab Med 2006; 130:1026–30.
4. Hicks DG, Tubbs RR. Assessment of the HER2 status in breast cancer by fluorescence *in situ* hybridization: a technical review with interpretive guidelines. Hum Pathol 2005;36:250–61.
5. Mischel PS, Cloughesy TF, Nelson SF. DNA-microarray analysis of brain cancer: molecular classification for therapy. Nat Rev Neurosci 2004;5:782–92.
6. Perez OD, Nolan GP. Simultaneous measurement of multiple active kinase states using polychromatic flow cytometry. Nat Biotechnol 2002;20:155–62.
7. Krutzik PO, Nolan GP. Fluorescent cell barcoding in flow cytometry allows high-throughput drug screening and signaling profiling. Nat Methods 2006;3:361–8.
8. Furnari FB, Fenton T, Bachoo RM, et al. Malignant astrocytic glioma: genetics, biology, and paths to treatment. Genes Dev 2007;21: 2683–710.
9. Ekstrand AJ, Sugawa N, James CD, Collins VP. Amplified and rearranged epidermal growth factor receptor genes in human glioblastomas reveal deletions of sequences encoding portions of the N- and/or C-terminal tails. Proc Natl Acad Sci U S A 1992; 89:4309–13.
10. Smith JS, Tachibana I, Passe SM, et al. PTEN mutation, EGFR amplification, and outcome in patients with anaplastic astrocytoma and glioblastoma multiforme. J Natl Cancer Inst 2001;93:1246–56.
11. Ermoian RP, Furniss CS, Lamborn KR, et al. Dysregulation of PTEN and protein kinase B is associated with glioma histology and patient survival. Clin Cancer Res 2002;8:1100–6.
12. Brachmann S, Fritsch C, Maira SM, Garcia-Echeverria C. PI3K and mTOR inhibitors: a new generation of targeted anticancer agents. Curr Opin Cell Biol 2009;21:194–8.
13. Mellinghoff IK, Cloughesy TF, Mischel PS. PTEN-mediated resistance to epidermal growth factor receptor kinase inhibitors. Clin Cancer Res 2007;13:378–81.
14. Mellinghoff IK, Wang MY, Vivanco I, et al. Molecular determinants of the response of glioblastomas to EGFR kinase inhibitors. N Engl J Med 2005;353:2012–24.
15. Betensky RA, Louis DN, Cairncross JG. Influence of unrecognized molecular heterogeneity on randomized clinical trials. J Clin Oncol 2002;20:2495–9.
16. El-Ali J, Sorger PK, Jensen KF. Cells on chips. Nature 2006;442: 403–11.
17. Kamei K, Guo S, Yu ZT, et al. An integrated microfluidic culture device for quantitative analysis of human embryonic stem cells. Lab Chip 2009;9:555–63.
18. Einav S, Gerber D, Bryson PD, et al. Discovery of a hepatitis C target and its pharmacological inhibitors by microfluidic affinity analysis. Nat Biotechnol 2008;26:1019–27.
19. VanDijken J, Kaigala GV, Lauzon J, et al. Microfluidic chips for detecting the t(4;14) translocation and monitoring disease during treatment using reverse transcriptase-polymerase chain reaction analysis of IgH-MMSET hybrid transcripts. J Mol Diagn 2007;9:358–67.
20. Fan AC, Deb-Basu D, Orban MW, et al. Nanofluidic proteomic assay for serial analysis of oncoprotein activation in clinical specimens. Nat Med 2009;15:566–71.
21. Jokerst JV, Raamanathan A, Christodoulides N, et al. Nano-bio-chips for high performance multiplexed protein detection: determinations of cancer biomarkers in serum and saliva using quantum dot bioconjugate labels. Biosens Bioelectron 2009;24:3622–9.
22. Fan R, Vermesh O, Srivastava A, et al. Integrated barcode chips for rapid, multiplexed analysis of proteins in microliter quantities of blood. Nat Biotechnol 2008;26:1373–8.
23. Huang B, Wu H, Bhaya D, et al. Counting low-copy number proteins in a single cell. Science 2007;315:81–4.
24. Cheong R, Wang CJ, Levchenko A. High content cell screening in a microfluidic device. Mol Cell Proteomics 2009;8:433–42.
25. Gordon A, Colman-Lerner A, Chin TE, Benjamin KR, Yu RC, Brent R. Single-cell quantification of molecules and rates using open-source microscope-based cytometry. Nat Methods 2007;4:175–81.
26. Kohonen T. The self-organizing map. Proc IEEE 1990;78:1464–80.
27. Wang MY, Lu KV, Zhu S, et al. Mammalian target of rapamycin inhibition promotes response to epidermal growth factor receptor kinase inhibitors in PTEN-deficient and PTEN-intact glioblastoma cells. Cancer Res 2006;66:7864–9.
28. Hemmati HD, Nakano I, Lazareff JA, et al. Cancerous stem cells can arise from pediatric brain tumors. Proc Natl Acad Sci U S A 2003; 100:15178–83.
29. Choe G, Horvath S, Cloughesy TF, et al. Analysis of the phosphatidylinositol 3′-kinase signaling pathway in glioblastoma patients *in vivo*. Cancer Res 2003;63:2742–6.
30. Wehrens R, Buydens LMC. Self- and super-organizing maps in R: the Kohonen package. J Stat Soft 2007;21:1–19.
31. Eisen MB, Spellman PT, Brown PO, Botstein D. Cluster analysis and display of genome-wide expression patterns. Proc Natl Acad Sci U S A 1998;95:14863–8.
32. Saldanha AJ. Java Treeview—extensible visualization of microarray data. Bioinformatics 2004;20:3246–8.
33. Lee ET, Wang JW. Statistical methods for survival data analysis. 3rd ed New York: Wiley; 2003.
34. Biernat W, Huang H, Yokoo H, Kleihues P, Ohgaki H. Predominant expression of mutant EGFR (EGFRvIII) is rare in primary glioblastomas. Brain Pathol 2004;14:131–6.
35. Krutzik PO, Nolan GP. Intracellular phospho-protein staining techniques for flow cytometry: monitoring single cell signaling events. Cytometry A 2003;55:61–70.
36. Freeman DJ, Li AG, Wei G, et al. PTEN tumor suppressor regulates p53 protein levels and activity through phosphatase-dependent and -independent mechanisms. Cancer Cell 2003;3:117–30.
37. Tamayo P, Slonim D, Mesirov J, et al. Interpreting patterns of gene expression with self-organizing maps: methods and application to hematopoietic differentiation. Proc Natl Acad Sci U S A 1999;96: 2907–12.
38. Huang PH, Mukasa A, Bonavia R, et al. Quantitative analysis of EGFRvIII cellular signaling networks reveals a combinatorial therapeutic strategy for glioblastoma. Proc Natl Acad Sci U S A 2007; 104:12867–72.
39. Wang J, Delabie J, Aasheim H, Smeland E, Myklebost O. Clustering of the SOM easily reveals distinct gene expression patterns: results of a reanalysis of lymphoma study. BMC Bioinformatics 2002;3:36.

40. Irish JM, Hovland R, Krutzik PO, et al. Single cell profiling of potentiated phospho-protein networks in cancer cells. Cell 2004;118: 217–28.

41. Irish JM, Kotecha N, Nolan GP. Mapping normal and cancer cell signalling networks: towards single-cell proteomics. Nat Rev Cancer 2006;6:146–55.

42. Murat A, Migliavacca E, Gorlia T, et al. Stem cell-related "self-renewal" signature and high epidermal growth factor receptor expression associated with resistance to concomitant chemoradiotherapy in glioblastoma. J Clin Oncol 2008;26:3015–24.

43. Yang J, Liao D, Wang Z, Liu F, Wu G. Mammalian target of rapamycin signaling pathway contributes to glioma progression and patients' prognosis. J Surg Res 2009.

44. Kotecha N, Flores NJ, Irish JM, et al. Single-cell profiling identifies aberrant STAT5 activation in myeloid malignancies with specific clinical and biologic correlates. Cancer Cell 2008;14: 335–43.

45. Brennan C, Momota H, Hambardzumyan D, et al. Glioblastoma subclasses can be defined by activity among signal transduction pathways and associated genomic alterations. PLoS One 2009;4:e7752.

46. Verhaak RG, Hoadley KA, Purdom E, et al. Integrated genomic analysis identifies clinically relevant subtypes of glioblastoma characterized by abnormalities in PDGFRA, IDH1, EGFR, NF1. Cancer Cell 2010;17:98–110.

47. Cloughesy TF, Yoshimoto K, Nghiemphu P, et al. Antitumor activity of rapamycin in a phase I trial for patients with recurrent PTEN-deficient glioblastoma. PLoS Med 2008;5:e8.

48. Laks DR, Masterman-Smith M, Visnyei K, et al. Neurosphere formation is an independent predictor of clinical outcome in malignant glioma. Stem Cells 2009;27:980–7.